0026-895X/05/6803-606–615$20.00
MOLECULAR PHARMACOLOGY
Copyright © 2005 The American Society for Pharmacology and Experimental Therapeutics
Mol Pharmacol 68:606–615, 2005

Vol. 68, No. 3
13474/3047146
Printed in U.S.A.

Vitamin K3 (Menadione)-Induced Oncosis Associated with Keratin 8 Phosphorylation and Histone H3 Arylation

Gary K. Scott, Christian Atsriku, Patrick Kaminker, Jason Held, Brad Gibson, Michael A. Baldwin, and Christopher C. Benz

Buck Institute for Age Research (G.K.S., C.A., P.K., J.H., B.G., M.A.B., C.C.B.), and Department of Pharmaceutical Chemistry (C.A., B.G., M.A.B.), University of California San Francisco, San Francisco, California

Received April 4, 2005; accepted June 3, 2005

ABSTRACT

The vitamin K analog menadione (K3), capable of both redox cycling and arylating nucleophilic substrates by Michael addition, has been extensively studied as a model stress-inducing quinone in both cell culture and animal model systems. Exposure of keratin 8 (k-8) expressing human breast cancer cells (MCF7, T47D, SKBr3) to K3 (50–100 μM) induced rapid, sustained, and site-specific k-8 serine phosphorylation (pSer73) dependent on signaling by a single mitogen activated protein kinase (MAPK) pathway, MEK1/2. Normal nuclear morphology and k-8 immunofluorescence coupled with the lack of DNA laddering or other features of apoptosis indicated that K3-induced cytotoxicity, evident within 4 h of treatment and delayed but not prevented by MEK1/2 inhibition, was due to a form of stress-activated cell death known as oncosis. Independent of MAPK signaling was the progressive appearance of K3-induced cellular fluorescence, principally nuclear in origin and suggested by in vitro fluorimetry to have been caused by K3 thiol arylation. Imaging by UV transillumination of protein gels containing nuclear extracts from K3-treated cells revealed a prominent 17-kDa band shown to be histone H3 by immunoblotting and mass spectrometry (MS). K3 arylation of histones in vitro followed by electrospray ionization-tandem MS analyses identified the unique Cys110 residue within H3, exposed only in the open chromatin of transcriptionally active genes, as a K3 arylation target. These findings delineate new pathways associated with K3-induced stress and suggest a potentially novel role for H3 Cys110 as a nuclear stress sensor.

Quinones encompass a broad array of biologically active compounds found both endogenously, as in the mitochondrial electron transporter ubiquinone, and exogenously, where studies have documented their diverse health risks as carcinogenic, immunotoxic, and cytotoxic agents (Bolton et al., 2000). As xenobiotic agents, quinones can disrupt cellular function via two distinct chemical pathways. Redox cycling quinones promote the generation of reactive oxygen species (ROS). Otherwise, as Michael acceptors, quinones covalently modify cellular nucleophiles, most prominently sulfur nucleophiles such as cysteine residues on proteins, creating potentially damaging arylation adducts. For quinones with both redox cycling and arylating potential, the contribution of each of these pathways to cellular stress response is difficult to fully quantify (Abdelmohsen et al., 2003; Schmeider et al., 2003).

The vitamin K analog menadione (K3) is capable of both redox cycling and arylation and thus serves as a model bifunctional quinone. Previous studies have demonstrated that K3 stimulates phosphorylation of the mitogen-activated protein kinase/extracellular regulated kinase (MAPK/Erk) pathway predominantly by arylation of key catalytic cysteine residues within protein tyrosine phosphatases (Osada et al., 2001; Klotz et al., 2002; Abdelmohsen et al., 2003). Although it is generally the case that this pathway serves to stimulate cell growth and survival, recent findings have implicated nonsurvival aspects to excessive MAPK activation (Osada et

This work was supported by National Institutes of Health grants R01-CA71468, R01-CA36773, and R01-AG020521; California Breast Cancer Research Program grant CBCRP 10YB-0125; NCRR-RR01614 facility grant support to the UCSF Mass Spectrometry Facility; and generous donations to the Buck Institute by the Oracle Corporate Giving Program and the Hazel P. Munroe Memorial.

Article, publication date, and citation information can be found at http://molpharm.aspetjournals.org.

doi:10.1124/mol.105.013474.

ABBREVIATIONS: ROS, reactive oxygen species; K3, vitamin K analog menadione; k-8, keratin 8; MAPK, mitogen-activated protein kinase; Erk, extracellular regulated kinase; JNK, c-Jun N-terminal kinase; HRP, Horseradish peroxidase; U0126, 1,4-diamino-2,3-dicyano-1,4-bis(2-aminophynyltio)butadiene; LY294002, 2-(4-morpholinyl)-8-phenyl-4*H*-1-benzopyran-4-one; DMNQ, 2,3-dimethoxy-1,4-naphthoquinone; SB203580, 4-(4-fluorophenyl)-2-(4-methylsulfinylphenyl)-5-(4-pyridyl)1*H*-imidazole; BQ, *p*-benzoquinone; NAC, *N*-acetyl cysteine; IAA, iodoacetic acid; DAPI, 4,6-diamidino-2-phenylindole; MOPS, 3-(*N*-morpholino)propanesulfonic acid; LC, liquid chromatography; ESI, electrospray ionization; MS/MS, tandem mass spectrometry; PI3K, phosphoinositide 3-kinase; ER, estrogen receptor; SP600125, 1,9-pyrazoloanthrone.

al., 2001; Tikoo et al., 2001; Choi et al., 2004; de Bernardo et al., 2004; Dong et al., 2004), including induction of a non-apoptotic form of cell death known as oncosis (Trump et al., 1997; Tikoo et al., 2001; Van Cruchte and Van Den Broeck, 2002; Romashko et al., 2003). Thus, identifying early molecular targets of K3-induced cell stress will improve our understanding of quinone effects on cell function and fate.

The human breast cancer cells used in this study express abundant keratin 8 (k-8) and keratin 18 (k-18) as major components of their cytoskeletal structure. Keratins, limited in expression to tissues of epithelial origin, comprise the largest group of intermediate filament proteins and undergo extensive reorganization and modification during such cellular responses as mitosis, apoptosis and stress (Liao et al., 1997). Although the functional consequences of keratin reorganization and post-translational modification remain poorly understood, some insights have emerged (Liao et al., 1997; He et al., 2002; Schutte et al., 2004). Previous studies have documented that the stress activated protein kinases c-Jun N-terminal kinase (JNK) and p38 kinase target Ser73 of k-8 for phosphorylation in response to a variety of cellular stresses and apoptosis inducing signals, whereas caspase cleavage of k-18 occurs as an early event during apoptosis thought to facilitate cellular breakdown (He et al., 2002; Ku et al., 2002; Schutte et al., 2004).

In this report, k-8 expressing breast cancer cells were studied after short-term K3 stress with the aim of uncovering biological targets mediating the cytotoxicity induced by this redox active and arylating quinone. K3 exposure was found to initiate rapid MEK1/2-dependent Ser73 phosphorylation of k-8 which was maintained at a steady-state level as cells progressively assumed the hallmark features of oncosis. Almost concurrent with k-8 phosphorylation was the appearance of K3-induced cellular fluorescence, which was primarily nuclear in origin and suggested by fluorimetry to reflect K3 thiol arylation. Evidence is presented implicating histone H3 as a prominent K3 arylation target.

Materials and Methods

Reagents. Antibodies used in this study included the k-8 pSer73 specific mouse monoclonal Ab-7 (clone LJ4), the mouse monoclonal Ab-4 specific for k-8 (clone TS1), and the mouse monoclonal Ab-8 (clone L2A1) specific for k-18; all were obtained from Lab Vision (Fremont, CA). Total Erk1/2 and pErk1/2 specific rabbit polyclonal antibodies were from Cell Signaling Technology Inc. (Beverly, MA). Phosphoserine antibodies were from Abcam (Cambridge, MA). Horseradish peroxidase (HRP)-coupled goat anti-mouse and HRP-coupled goat anti-rabbit antibodies were from Bio-Rad (Hercules, CA). Alexa Fluor 488 goat anti-mouse was from Molecular Probes (Eugene , OR). U0126, LY294002, DMNQ, and SB203580 were from Calbiochem. SP600125 was from A.G. Scientific (San Diego, CA). Menadione (K3), *p*-benzoquinone (BQ), histones, cysteine, *N*-acetyl cysteine (NAC), glutathione, iodoacetic acid (IAA), and trypan blue were all obtained from Sigma (St. Louis, MO).

Cell Lines, Treatment Conditions, and Cell Viability Assessment. Human breast cancer cell lines MCF7, T47D, and SKBr3 were obtained from the American Type Culture Collection (Manassas, VA). MCF7 cells were maintained in Dulbecco's modified Eagle's medium (Mediatech, Inc., Herndon, VA) supplemented with 10% fetal bovine serum (Mediatech), 1% penicillin/streptomycin (Mediatech), and 10 μg/ml insulin (Sigma). T47D cells were maintained in RPMI medium (Mediatech) supplemented with 10% fetal bovine serum, 1% penicillin/streptomycin, and 10 μg/ml insulin. SKBr3 cells were maintained in McCoy's buffer (Mediatech) supplemented with 10% fetal bovine serum and 1% penicillin/streptomycin. Treatment conditions for all cell lines involved plating $\sim 1 \times 10^6$ cells in normal media onto 10-cm dishes, attachment and growth for 24 h, followed by a change to estrogen-free culture conditions (phenol red-free Dulbecco's modified Eagle's medium–H-16 supplemented with 10% charcoal stripped serum, 1% penicillin/streptomycin, and 10 μg/ml insulin) for an additional 24 h to eliminate any potential estrogen stimulatory influences or estrogen metabolism to catechols and quinones. Cells were then treated as indicated before fractionation and extract preparation. Cell viability was assessed at timed intervals after initiation of culture treatment using 12-well culture dishes containing $\sim 40 \times 10^3$ cells per well. Replica-plated for each treatment condition, wells were stained with Trypan Blue and cells were scored for dye exclusion, counting at least 1500 cells per well from representative areas. Separate experiments assessing cell viability were repeated at least three times.

Immunofluorescence and Microscopy. Cells were plated, grown, and treated as described above on Lab-Tek II Chamber Slides (Nalge Nunc Internationa, Naperville, IL). To image k-8 by immunofluorescence, cells were permeabilized with 0.5% Triton X-100 (Sigma), fixed with 4% paraformaldehyde (Sigma), and blocked with 5% normal goat serum (Rockland Immunochemicals, Gilbertsville, PA) for 1 h in wash buffer (10 mM Tris, pH 7.5, 150 mM NaCl, and 1% bovine serum albumin). Fixed, permeabilized, and blocked cells were first incubated with the k-8 (Ab-4) or the k-8 pSer73 antibody (Ab-7) at 1:300 dilution for 1 h at room temperature in wash buffer containing 2.5% goat serum and then incubated for 1 h at room temperature with a fluorescent goat anti-mouse secondary (Alexa Fluor 488; Molecular Probes) in wash buffer containing 2.5% goat serum. Nuclear DNA was imaged by DAPI staining (0.5 μg/ml), and slides were mounted (Vector Laboratories), viewed, and photographed using a Nikon E800 upright fluorescence microscope equipped with excitation (Ex)/emission (Em) filters: (Ex 480 nm/Em 535 nm), (Ex 535 nm/Em 610 nm), and (Ex 360 nm/Em 460 nm). For immunofluorescence studies not employing primary or secondary antibodies, treated and control cells grown in Lab-Tek II Chamber Slides were permeabilized with 0.5% Triton X-100 (Sigma) in PBS, fixed with 4% paraformaldehyde (Sigma), then washed extensively with multiple phosphate-buffered saline changes. DNA was visualized by addition of DAPI (0.5 μg/ml) except in those experiments in which its omission was noted and slides were mounted, viewed, and photographed as described above.

Cell Fractionation, Nuclear Extracts, and Genomic DNA Analysis. After aspiration of culture media and one ice-cold PBS wash, cells growing on 10-cm dishes were harvested using a cell scraper and 0.7 ml of ice-cold cell lysis buffer (10 nM HEPES, pH 7.9, 1.5 mM $MgCl_2$, 10 nM KCl, 1 mM dithiothreitol, 10 nM NaFl, 5% glycerol, 0.45% Nonidet P-40, and Roche mini-Complete protease inhibitor cocktail). Nuclei with insoluble cytoplasmic components were pelleted at 4°C in a microcentrifuge for 4 min at 3000*g*. The supernatant constituted the soluble cytosol, whereas the pelleted material was resuspended in 90 μl of DNase I digestion buffer (20 mM Tris, pH 7.5, 100 nM NaCl, and 10 mM $MgCl_2$) and incubated with 300 units of DNase I at room temperature for 5 min. After DNase I digestion, complete solubilization of the pelleted material was achieved by addition of SDS (to 1%) to the DNase I reaction. Acid extraction of the pelleted fraction was performed with 0.2 M HCl. Aliquots of the acid extracted material were treated with 1 mM K3 for 1 h at 25°C and then neutralizaion with 0.5 Tris pH 11 before protein gel electrophoresis. Genomic DNA was extracted and analyzed for DNA laddering as follows. Control and treated cells were harvested in buffer (20 mM Tris pH 7.5, 50 mM EDTA, 100 mM NaCl, 0.5% SDS, and 200 μg/ml Proteinase K), incubated at 56°C for 5 h, phenol/chloroform-extracted, ethanol-precipitated, and resuspended in Tris-EDTA buffer with the addition of RNase A to remove background RNA. The resulting genomic DNA was electrophoresed on a 1% agarose gel using 1× Tris-borate/EDTA. As a positive control

for DNA laddering, genomic DNA was prepared from cultured SKBr3 induced into apoptosis by 6 h treatment with conditioned media from cultures grown 5 days beyond confluence.

Western Analyses. Equal amounts of protein from the various treatments were mixed with 2× SDS sample buffer (125 mM Tris, pH 6.8, 20% glycerol, 2% SDS, 0.28 M 2-mercaptoethanol, and 0.5% bromphenol blue), heated for 5 min at 90°C and electrophoresed on Nu-PAGE 4 to 12% Bis-Tris gels (Invitrogen, Carlsbad, CA) using NuPAGE MOPS SDS running buffer (Invitrogen) and full-range Rainbow recombinant protein molecular mass markers (Amersham Biosciences, Piscataway, NJ). Gels were electroblotted onto Hybond ECL nitrocellulose membranes (Amersham Biosciences) in standard transfer buffer (25 mM Tris and 200 mM glycine with 20% methanol) at 250 mA for 1 h at room temperature. Membranes were then blocked for 30 min in blocking buffer (150 mM NaCl, 20 mM Tris, pH 7.5, 0.3% Tween 20, and 4% nonfat dry milk powder by weight). After blocking, membranes were incubated overnight at 4°C with the primary antibody in blocking buffer using a 1:1000 dilution of the supplied antibody concentration. Membranes were then washed three times for 5 min each in blocking buffer without the milk powder, incubated with an HRP-conjugated secondary antibody at 1:10,000 dilution in blocking buffer for 1 h at room temperature, and washed three times for 10 min each in blocking buffer without dry milk power. Membranes were then developed using SuperSignal West Pico Chemiluminescent substrate (Pierce) according to the manufacturer's instructions.

Fluorimetry and Fluorescence Illumination of Gel-separated Proteins. K3 stock (0.1 M in dimethyl sulfoxide) was diluted to 1 mM in either water or a 50:50 ethanol/water mixture for fluorimetry using a luminescence spectrometer (model LS50B; PerkinElmer Life and Analytical Sciences, Boston, MA). To induce K3 thioether formation, K3 from stock solution was added directly to 100 mM cysteine or 100 nM glutathione solutions in water to a final 1 mM K3 concentration. After allowing the reaction to proceed for 10 min at room temperature, the mixture was analyzed in the spectrometer at the indicated excitation and emission wavelengths. For analysis of cell lysates, 100 μl of nuclear lysate (standardized for equal protein content) treated with vehicle or K3 stock was diluted after treatment with 400 μl of water and analyzed in the spectrometer. For fluorescence detection of gel-separated proteins, extracts prepared as described above were gel separated as for Western analyses, washed extensively in water after electrophoresis, imaged using an Epi ChemiII Darkroom UV transilluminator (UVP, Inc., Upland, CA), and photographed using a SYBR Green filter (515 nm–570 nm) with fully opened aperture and a 7-s exposure time.

Histone Derivatization and Mass Spectrometry. A stock solution of commercially acquired human histones (Sigma; 10 μg/μl) was prepared in water, and a 2-μl aliquot of the stock solution was either untreated (control) or treated with K3 to a final concentration of 3 mM in an acid environment [0.5% acetic acid (v/v)] for 1 h at 37°C. After a 2-fold dilution with ammonium bicarbonate (pH 8, 25 mM), the control and K3-treated samples were treated with dithiothreitol (4 mM) to reduce any disulfide bonds, followed by addition of iodoacetic acid (6 mM) for alkylation of cysteine thiols (control) or alkylation of any remaining cysteine thiols that were not arylated by the initial K3 treatment. The samples were then diluted 10-fold with ammonium bicarbonate followed by digestion with trypsin (20 ng/μl) and a second endoproteinase, Asp-N (40 ng/μl). Mixtures of derivatized peptides were desalted and concentrated using C-18 ziptips (Millipore, Billerica, MA) for subsequent mass spectrometric analysis. Liquid chromatography-electrospray ionization-tandem mass spectrometry (LC-ESI-MS/MS) was performed using a QSTAR Pulsar mass spectrometer (Applied Biosystems/MDS Sciex, Foster City, CA) operated in the positive-ion mode with a nano-electrospray needle voltage of 2300 V. Loading and elution of peptides onto the LC column was performed using a binary solvent system: solvents A (0.05% formic acid in 98% H_2O/2% AcN) and B (0.05% formic acid in 2% H_2O/98% acetonitrile) at a flow rate of 300 nl/min and a gradient of 2% solvent B (from 0–5 min), and then 2 to 70% solvent B (from 5–55 min). Data (MS and tandem MS) were recorded continuously, peak lists for database searching were created using a script from within Analyst software, and peptide sequences were identified using an in-house version of the database search package Protein Prospector (http://prospector.ucsf.edu/). Database searches were performed by preselecting K3- or IAA-modified amino acid residues of cysteine and/or lysine incorporated in the Protein Prospector software.

Results

K3 Rapidly Induces k-8 Ser73 Phosphorylation. Previous studies had documented the activation of MAPK (Erk1/2, p38, JNK) and PI3K/Akt signaling in response to quinone exposure (Klotz et al., 2002; Osada et al., 2002; Seanor et al., 2003). An intensely reactive band at 52 kDa was detected with the use of phosphoserine-specific antibodies to screen for proteins serine-phosphorylated after K3 treatment; it was subsequently identified by MS to be k-8. To further explore this response and eliminate potentially confounding effects from exogenous estrogens or endogenous quinone metabolites of estrogen, estrogen receptor (ER)-positive MCF7 cells were cultured in phenol-free media supplemented with charcoal-stripped serum for 24 h before 30 min K3 (100 μM) treatment. Parallel cultures were treated with an equimolar dose of the structurally similar redox-cycling and nonarylating quinone DMNQ. Harvested monolayer cells were lysed in hypotonic buffer and separated into two components, a soluble cytoplasmic fraction (Cyto) and a pellet fraction (Nu) containing intact nuclei and insoluble keratin filaments. As shown in Fig. 1B, the majority of k-8, despite being a cytoplasmic protein, pelleted predominantly as insoluble filaments, with only a small soluble pool remaining in the cytoplasmic fraction (Chou et al., 1993). Using monoclonal antibodies against k-8 and k-8 pSer73, Fig. 1A shows that K3 significantly increased k-8 pSer73 above control levels, whereas DMNQ treatment produced only a small increase in k-8 pSer73. Comparison of the Cyto and Nu fractions showed that the majority of k-8 pSer73 was present in the insoluble filamentous Nu fraction, as shown in Fig. 1B. The localization of Erk1/2 primarily within the Cyto fraction confirmed the efficiency of the separation protocol (Fig. 1B). Titration of K3 concentrations demonstrated a sharp decline in k-8 pSer73 formation below 50 μM, with $\leq$10 μM K3 producing little or no k-8 pSer73 relative to K3 doses $\geq$50 μM, as shown in Fig. 1C. In addition, nearly maximal k-8 pSer73 levels occurred within 0.5 h of K3 exposure and remained unabated even after 6 h of treatment (Fig. 1D). In two other human breast cancer cell lines, ER-negative SKBr3 and ER-positive T47D, 100 μM K3-induced k-8 pSer73 formation in a manner similar to that seen with MCF7 (data not shown).

To examine potential changes in MCF7 cytoskeletal architecture induced by K3 treatment, total k-8 and k-8 pSer73 were imaged by fluorescence microscopy. As shown in Fig. 2, k-8 containing cytoplasmic filaments were evident before treatment and remained relatively unchanged even 3 h after K3 (100 μM) treatment. In contrast, strong induction of k-8 pSer73 was seen in well defined cytoplasmic filaments within 3 h of K3 treatment, and minimal k-8 pSer73 was apparent in untreated MCF7 cells.

MEK1/2 Inhibition Prevents K3-Induced k-8 pSer73 and Delays the Onset of K3 Cytotoxicity. To determine which signaling pathway(s) mediate K3 induction of k-8 pSer73, human breast cancer cells were pretreated for 10 min with inhibitors of MEK1/2 (10 μM U0126), p38 (10 μM SB203580), JNK (30 μM SP600125), or PI3K/Akt (10 μM LY294002) before the addition of K3 (100 μM $\times$ 30 min). As shown in Fig. 3A, the MEK1/2 inhibitor reduced k-8 pSer73 phosphorylation to control levels, whereas the p38, JNK, and PI3K/Akt inhibitors had no impact on K3-induced k-8 pSer73. Also shown in Fig. 3A was the suppression of K3-induced k-8 pSer73 resulting from concurrent treatment of cells with the thiol donor and arylation quencher *N*-acetyl cysteine (NAC), a result consistent with previous observations (Abdelmohsen et al., 2003). Confirmation that the immediate downstream targets of MEK1/2 signaling, Erk1/2, were phosphorylated by K3-induced MEK1/2 activation and that this activation was inhibited by U0126 pretreatment is shown Fig. 3B. In addition, Fig. 3 confirms the inhibition by NAC of K3-induced MEK1/2 activation. DMNQ, which produced a slight increase in k-8 pSer73 (Fig. 1A), induced activation of Erk1/2, albeit not to the degree elicited by K3 (Fig. 3B).

Because activation of the MAPK pathway and k-8 pSer73 have been associated with cellular stress, and U0126 prevented K3-induced Erk1/2 and k-8 phosphorylation, the ability of U0126 (10 μM) to prevent K3 (100 μM) induced cytotoxicity was examined by measuring MCF7 cell viability at hourly intervals after K3 treatment. As shown in Fig. 3C, inhibition of Erk1/2 and k-8 phosphorylation extended cell viability by as much as 25% after 3 to 4 h of K3 treatment relative to cells that did not receive U0126 cotreatment; however, by 6 h after K3 treatment, there was virtually complete loss of MCF7 cell viability regardless of U0126 cotreatment. The morphological features of all breast cancer cell lines examined (MCF7, SKBr3, T47D) showed comparable loss of cell viability within 6 h of K3 treatment without evidence of any typical features of apoptosis such as membrane blebbing, cell shrinkage, chromatin condensation, or DNA fragmentation. Adherent but nonviable K3-treated cells

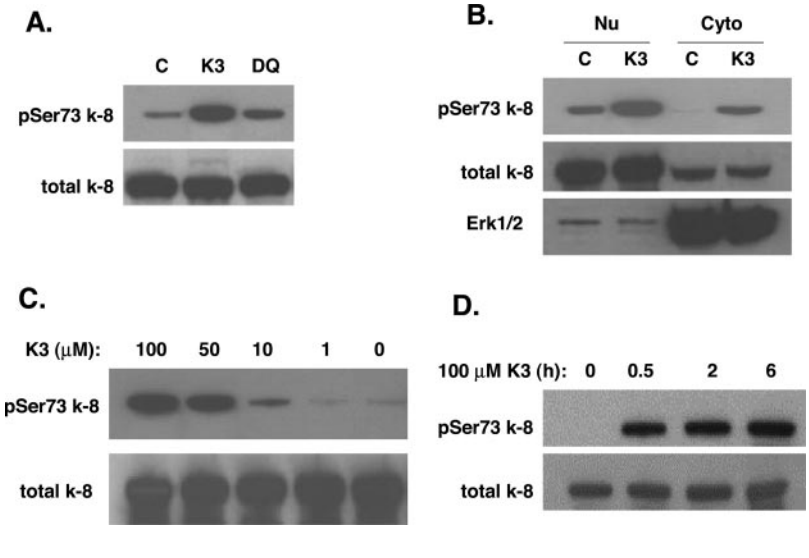

Fig. 1. Menadione (K3) induces Ser73 phosphorylation of keratin 8 (pSer73 k-8) in MCF7 cells. A, Western blots of MCF7 nuclear pellet fractions (also containing insoluble cytoplasmic keratin filaments) from vehicle-treated control cultures (C) and cultures treated with 100 μM K3 or DMNQ (DQ) for 30 min. As shown, immunoblots were probed with antibodies specific for total k-8 or pSer73 k-8. B, Western blots of nuclear pellets (Nu) or soluble cytosols (Cyto) from MCF7 cultures treated as in A and probed with antibodies for total k-8, pSer73 k-8, or Erk1/2 (42/44 kDa). C, Western blots of nuclear pellets from MCF7 cultures treated for 30 min with the indicated concentrations of K3 and probed as indicated. D, Western blots of nuclear pellets from MCF7 cultures treated with 100 μM K3 for the indicated times (h) and probed as shown.

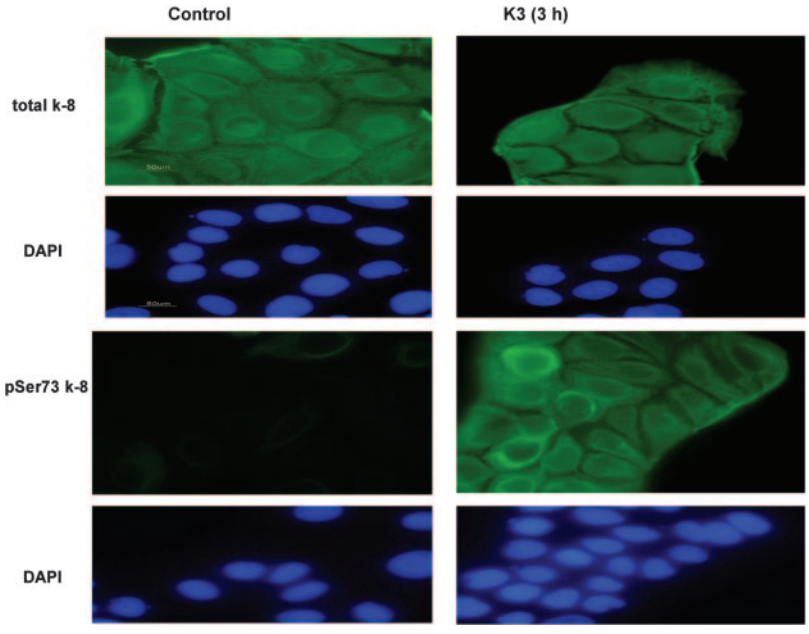

Fig. 2. Immunocytochemical detection of k-8 and pSer73 k-8. Control and 3-h K3-treated MCF7 cells were immunocytochemically examined by fluorescence microscopy for total k-8 (top) and pSer73 k-8 (bottom) expression. An exposure time of 0.06 s was used to obtain total k-8 and pSer73 k-8 fluorescence images. DAPI staining was used to distinguish MCF7 nuclei.

all retained their cytoplasmic k-8 filamentous structures, nuclear contours, and normal-appearing DAPI-stained chromatin; upon examination of their genomic DNA, treated cells showed some evidence of DNA degradation but no evidence of the DNA laddering that signifies apoptosis (Fig. 3D). Observed light microscopic changes in cell morphology associated with K3 cytotoxicity were most consistent with oncosis (Trump et al., 1997; Van Cruchte and Van Den Broeck, 2002), the cell death pathway induced by various physical and chemical stresses and characterized by swelling of intracellular organelles, including mitochondria and nucleoli, and development of a refractive fringe around cell margins because of loss of plasma membrane integrity and cell junctions.

Rapid Induction of Nuclear Fluorescence Consistent with K3 Thiol Arylation. Fluorescence microscopy revealed that K3-treated breast cancer cells rapidly became fluorescent, most prominently within the nucleus, whereas no comparable fluorescence was evident in vehicle-treated control cells. Although the capacity of K3 to modify thiol groups through arylation has been well documented (Toxopeus et al., 1993; Feng et al., 1999; MacDonald et al., 2004), we are aware of no reports describing K3-induced cellular fluorescence. After detergent (0.5% triton) permeabilization to remove soluble cell components and fixation in paraformaldeyde (4%), K3-treated (100 μM) MCF7 cells acquired diffusely intense nuclear fluorescence when excited at 480 nm and imaged at 535 nm or when excited at 535 nm and imaged at 640 nm (Fig. 4). It is noteworthy that the K3-induced nuclear fluorescence viewed over 0.3 s left the k-8 immunofluorescence imaged over 0.07 s essentially undistorted (Fig. 2). This nuclear fluorescence seemed to increase in a relatively linear manner after K3 administration; emission intensity at 3 h seemed 3- to 4-fold greater than that seen after 0.5-h treatment and exceeded control autofluorescence by more than an order of magnitude (Fig. 4). The linear time course of K3-induced nuclear fluorescence that emerged over several hours contrasts with the kinetics of k-8 pSer73 formation, which reached maximal steady-state levels within 1 h (Fig. 1D). That protein arylation by K3 accounted for this nuclear fluorescence is supported by three observations. First, detergent permeabilization followed by paraformaldehyde fixation allowed for the elimination of soluble factors including unreacted K3 and soluble K3 complexes. Second, treatment with DMNQ, which is incapable of arylation, produced no cellular florescence above untreated cell autofluorescence (data not shown). Third, both K3-induced k-8 phosphorylation and K3-induced nuclear fluorescence were reduced to control levels by concurrent cell treatment with the thiol donor NAC, as shown in Figs. 3A and 4, respectively.

To examine the excitation and emission properties of fluorescence induced by various K3-arylated products, in vitro fluorimetry studies were preformed using cysteine and glutathione as soluble thiol donors. Unreacted K3 exhibited minimal fluorescence with best results attained with 340 nm excitation, which produced a poorly defined emission peak centered at 420 nm (Fig. 5, A and B). In contrast, after the virtually instantaneous reactions (at room temperature) between K3 and either cysteine or glutathione, strong K3 thioether emission peaks at 480 nm with 340 nm excitation and at 420 nm with 360 nm excitation were observed for cysteine and glutathione, respectively (Fig. 5, A and B). This >10-fold enhancement in K3 thioether fluorescence over un-

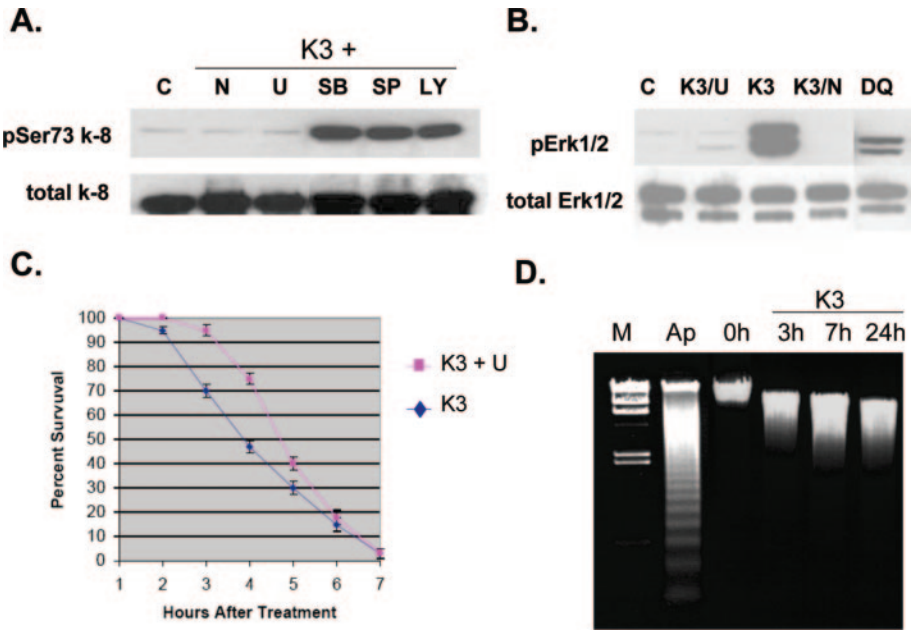

Fig. 3. MAPK dependence of K3 effects on pSer73 k-8, pErk1/2, cell survival and DNA integrity. A, Western blots of the nuclear pellets from MCF7 cultures treated for 30 min with 100 μM K3 and the indicated agents (C, vehicle control; U, 10 μM U0126; SB, 10 μM SB203580; SP, 30 μM SP600125; LY, 10 μM LY294002; N, 10 mM *N*-acetyl cysteine), and probed with antibodies as described in Fig. 1. B, Western blots of nuclear pellets from MCF7 cultures treated for 30 min with 100 μM K3 ($\pm$ cotreatment with 10 μM U0126), 100 μM K3 with 10 mM NAC (K/N), or 100 μM DMNQ (DQ), and then probed with antibodies to total or phosphorylated Erk1/2 (42/44 kDa). C, survival of MCF7 cells from cultures treated for the indicated times (hours) with 100 μM K3 with or without 10 μM U0126, as measured by trypan blue dye exclusion. Error bars represent S.E. from three replica plated experiments. D, ethidium-stained DNA agarose gel of genomic DNA isolated from SKBr3 cells treated in culture for 3 to 24 h with 100 μM K3. As a positive control for SKBr3 apoptosis, cells were exposed for 6 h to an apoptosis-inducing conditioned media (Ap) to demonstrate induction of DNA laddering. HindIII-digested lambda phages were used as DNA size markers (M).

reacted K3 was observed in both water and 50:50 water/ethanol vehicle, assuring that the low aqueous solubility of K3 was not biasing the fluorimetry results (data not shown). No fluorescence was detected from cysteine or glutathione without addition of K3. In near agreement with the K3-glutathione thioether fluorescence properties, a nuclear protein extract from cells treated with K3 (100 μM $\times$ 3 h) produced a strong fluorescence emission peak at 390 nm relative to untreated control extract with 340 nm excitation (Fig. 5C). These in vitro studies demonstrate that K3 expe-

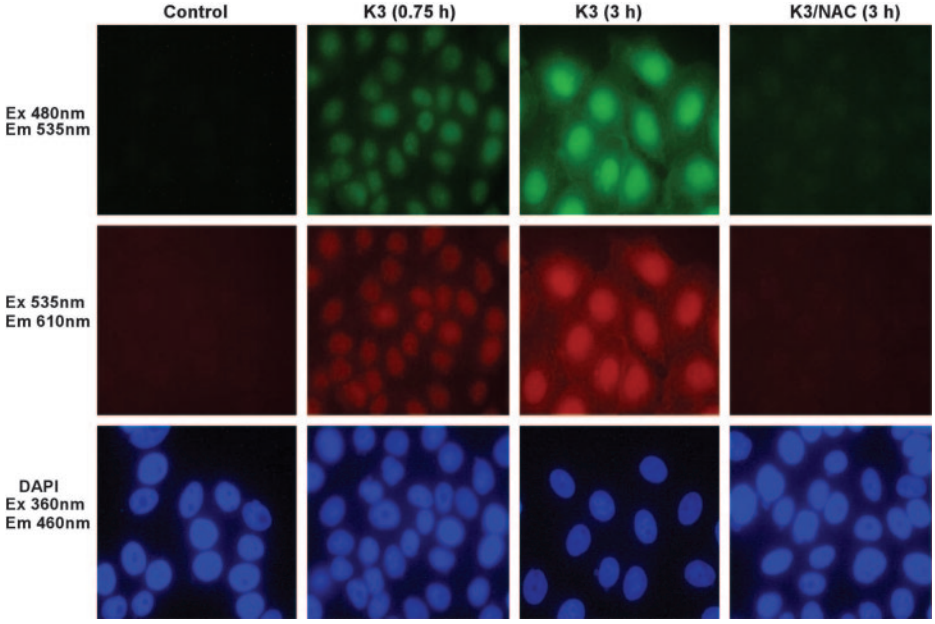

Fig. 4. Fluorescence microscopy of K3-treated MCF7 cells. Control; 0.75-h 100 μM K3-treated; 3-h 100 μM K3-treated; or 3-h 100 μM K3- and 10 mM NAC- treated (K3/NAC) MCF7 cells were imaged by fluorescence microscopy using an exposure time of 0.30 s for detection by filtering with excitation at 480 nm/emission at 535 nm (top) and an exposure time of 0.25 s for detection by filtering with excitation at 535 nm and emission at 610 nm (middle). DAPI fluorescence was used to image MCF7 nuclei (bottom).

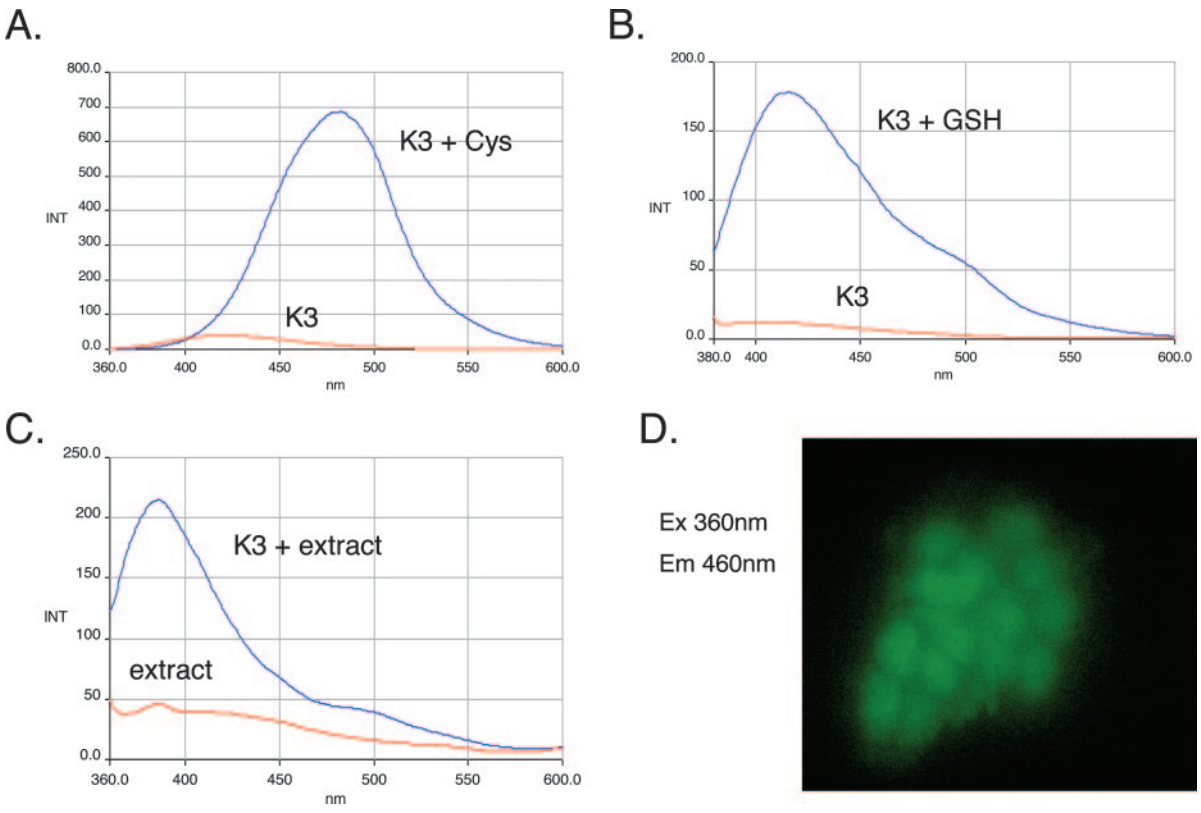

Fig. 5. K3 fluorescence after K3 thioether formation simulates the nuclear fluorescence from K3 treated MCF7 cells. A, emission spectra of 1 mM K3 (red line) in water or in the presence of 0.1 M aqueous cysteine solution (blue line), excited at 340 nm. B, emission spectra of 1 mM K3 (red line) in water or in the presence of 0.1 M aqueous glutathione (GST) solution (blue line), excited at 360 nm. C, emission spectra of solubilized nuclear pellet from MCF7 cell cultures treated with vehicle alone (Control Extract, red line) or for 3 h with 100 μM K3 (K3 Extract, blue line), excited at 340 nm. D, fluorescent microscopy of MCF7 cells treated for 3 h with 100 μM K3 and prepared as described in Fig. 4, except that the elimination of DAPI staining was imaged by filtering with excitation at 360 nm and emission at 460 nm and an exposure time of 0.3 s. The image is shown using green false coloring.

riences a >10-fold enhancement in fluorescent activity upon thioether formation, an observation that strengthens the conjecture that the K3-induced nuclear fluorescence observed in Fig. 4 results from K3 thioether formation. To simulate in a cellular environment these in vitro studies, which demonstrated excitation of the K3 thioether around 360 nm, monolayer MCF7 cells were treated with K3 for 3 h and then prepared similarly to those shown in Fig. 4 except that staining with DAPI, which absorbs at 360 nm, was eliminated. The cells were then analyzed by fluorescence microscopy using 360 ± 20 nm excitation and imaged at 460 ± 25 nm for 0.3 s (Fig. 5D). Although no fluorescence was detected in untreated cells, K3-treated cells demonstrated a diffuse and predominantly nuclear fluorescence pattern similar to that shown in Fig. 4.

Histone H3 Is the Major Nuclear Target of K3 Thiol Arylation. To identify protein targets of K3 arylation, nuclear extracts from K3-treated cells were resolved on protein gels and examined for fluorescent bands. After electrophoretic separation of control and K3-treated MCF7 extracts, polyacrylamide gels were thoroughly washed with water then imaged using a wide spectrum UV transilluminator coupled to a SYBR green filter (515–570 nm). Coomassie staining was subsequently performed to establish equal protein loading and molecular mass sizes. As shown in Fig. 6, strongly UV-illuminated protein bands were apparent in the K3-treated extracts, but only faintly detected bands were apparent in the untreated control nuclear extracts. Careful alignment of the UV transilluminated image with the Coomassie stained image revealed prominent K3-induced bands at 47, 43, and 17 kDa (Fig. 6). The intensely staining Coomassie bands at 52 kDa, corresponding to k-8, and 48 kDa, verified as k-18 by antibody (data not shown), were not accompanied by any detectable bands under UV transillumination. Of the K3-induced UV transilluminated bands, only the 17-kDa species precisely aligned with a strong Coomassie band. As nuclear proteins of this molecular size and abundance are predominantly histones, antibodies were used to confirm that the strong Coomassie bands at 11, 15, and 17 kDa corresponded to histones H4, H2a/H2b, and H3.3/H3, respectively (data not shown). Because H3 and its variants are the only histones that contain any cysteine residues (Cys110), the observed UV transilluminated protein within the 17-kDa band was most probably attributable to K3-induced thiol arylation of H3.3/H3. Supporting evidence for this proposal was obtained from in vitro K3 (1 mM) treatment of an acid extract of MCF7 nuclear pelleted material. As shown in Fig. 6, comparison of the in vivo and in vitro K3-treated nuclear proteins with their untreated controls showed similar Coomassie banding across all lanes, whereas UV transillumination revealed the 17-kDa H3.3/H3 band most prominently only in the K3-treated lanes.

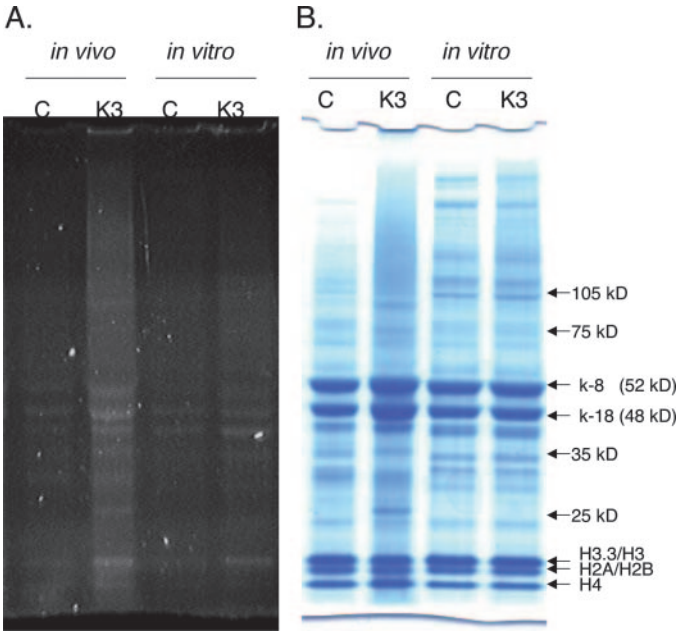

Fig. 6. K3 modified histone H3 detected by UV transillumination. Gel-separated proteins from the nuclear pelleted material of control (C) or 3 h 100 μM K3-treated (K3) MCF7 cells (in vivo) or from the acid-extracted nuclear pelleted material from control MCF7 cells (in vitro) treated with 1 mM K3 (K3) or untreated (C) were photographed for 7 s using a UV transilluminator equipped with a SYBR Green (515 nm–570 nm) filter (left). Continued exposure of the gel to UV transillumination resulted in the gradual appearance of bands in both K3 and C lanes. Precise alignment of the Coomassie stained protein gel image (right) with UV transilluminated image identified the 17-kDa histone H3/H3.3 Coomassie band as aligning with a prominent UV-stimulated band in K3 lanes. Molecular mass markers and known histone (H3, H2A/H2B, H4) and keratin (k-8, k-18) bands are indicated.

Histone H3 and its variant H3.3, which preferentially associates with transcriptionally active chromatin (McKittrick et al., 2004), are structurally identical except for four neutral amino acid differences within a short (10 amino acid) region adjacent to the conserved core domain containing Cys110 (Fig. 7A). Typically buried in the interior of the nucleosome, this C-terminal Cys110 for both H3.3/H3 becomes chemically accessible and reactive only during active gene transcription or other situations promoting open chromatin configuration (Arents et al., 1991; Bazett-Jones et al., 1996; Sun et al., 2002). ESI-MS/MS was used to confirm the ability of K3 to arylate H3.3/H3 at the thiol of Cys110. After IAA treatment of control and K3-treated histones from a commercial preparation, sequential protease digestion by trypsin and AspN was used to release the fragment 106-DTNLCAIHAK-115 from H3.3/H3. K3 quinone modification to Cys110 would be expected to increase the molecular mass of 106–115 peptide from 1084.5 to 1254.5 Da if arylated with K3. An electrophilic attack of a quinone-like K3 on a thiol moiety initially results in the reduction of the quinone to a dihydroquinone, but under aerobic conditions, this dihydroquinone is rapidly oxidized partially or completely back to the quinone. In addition, IAA modification of Cys110 in the control sample as well as to those Cys110 not modified by K3 in the K3-treated sample is expected to produce an IAA modified 106–115 peptide with a molecular mass of 1142.5 Da. As shown in Fig. 7B, I and III, for control and K3-treated samples, respectively, ESI-MS/MS identified a well defined peak at 1142.5 Da (381.85^{+3} *m/z*), corresponding to the anticipated mass of the IAA Cys110 modified 106–115 H3/H3.3 peptide fragment. However, as shown in Fig. 7B, II and IV, for control and K3-treated samples, respectively (note that the scale factor for II is reduced approximately 100-fold relative to IV), ESI-MS/MS detected a well defined peak at 1254.5 Da (419.17^{+3} *m/z*) corresponding to the presence of a Cys110 K3 modified 106–115 peptide only in the K3-treated histone sample. To precisely confirm the expected chemical alterations occurring on Cys110, selection and fragmentation of the IAA-modified 381.85^{+3} *m/z* ion and the K3-modified

419.17^{+3} ion by MS/MS yielded multiple y (C-terminal) and b (N-terminal) ion series as shown in Fig. 8, A and B, respectively. The 161-Da difference between the y_6 (700.3 *m/z*) and y_5 (539.3 *m/z*) ions shown in Fig. 8A reflects a single IAA moiety coupled to the Cys110 residue (103 Da), whereas the 273-Da difference between the y_6 (812.3 *m/z*) and y_5 (539.3 *m/z*) ions shown in Fig. 8B reflects a single K3 moiety coupled to Cys110. A similar ESI-MS/MS approach was attempted to detect K3 arylated H3.3/H3 from a digest performed on the 17-kDa protein band excised from gel separated nuclear extract of in vivo-treated K3 MCF7 cells. Although ESI-MS/MS analysis produced 80% sequence coverage of H3.3/H3, including successful detection of the Cys110-containing fragment (data not shown), K3-modified Cys110 was not detected, probably reflecting the relatively low abundance of K3 modified to unmodified H3.3/H3. In addition, because the 22-amino acid peptide fragment containing the four amino acids that distinguish H3 from H3.3 (Fig. 7A) was not detected, any Cys96 modifications occurring to H3 would have escaped identification.

Discussion

Although previous studies have shown activation of the MAPK pathway by both redox-cycling and arylating quinones (Osada et al., 2001; Klotz et al., 2002; Abdelmohsen et al., 2003; Seanor et al., 2003), the spectrum of quinone-targeted intracellular substrates remains largely uncharacterized. Results presented here demonstrate in human breast cancer cells (MCF7, T47D, SKBr3) that aberrant activation of MEK1/2 by the model quinone and vitamin K analog K3 leads to sustained Ser73 phosphorylation of k-8, a primary intermediate filament constituent of all simple epithelial cells that heterodimerizes with its obligate cytokeratin partner, k-18. In conjunction with this cytoplasmic event, we demonstrated that K3 induces nuclear fluorescence re-

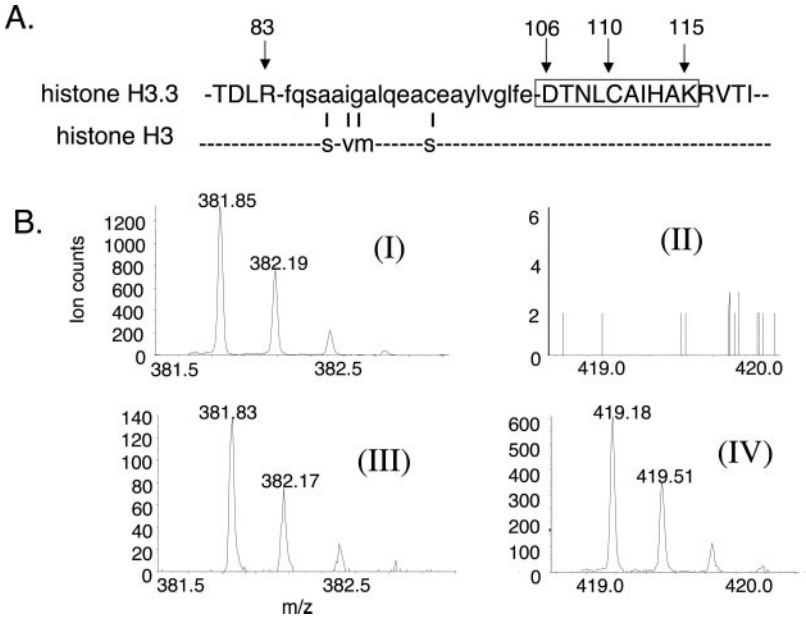

Fig. 7. MS detection of K3 thiol arylated or carboxymethylated peptide within histone H3.3/H3. A, primary structure of histones H3.3 and H3 in the region of interest showing the four amino acids distinguishing the two isoforms. Amino acids from 84 to 105 are shown in small type and were not detected by MS; amino acids detected by MS are shown in large type. The boxed peptide (amino acids from 106–115) contains the K3 or IAA-modified Cys110 detectable after H3.3/H3 double digestion with trypsin and Asp-N. B, LC-ESI-MS data for the IAA-treated negative controls (I and II) and the K3 treated histone conditions (III and IV). I and III show the triply charged ion (381.85^{+3} *m/z* peak) eluted at 19.7 min and corresponding to the carboxymethylated 106–115 peptide resulting from IAA treatment. II and IV show the signal for the analogous ion (419.18^{+3} *m/z* peak as well as its isotopic variants at 419.51 and 419.83, evident only in IV) eluted at 28.2 min and corresponding to the K3-adducted 106–115 peptide. In contrast to the prominent 419.18^{+3} *m/z* peak evident in IV, note the absence of any 419.18^{+3} *m/z* peak in II and the nearly 100-fold lower ordinate scale.

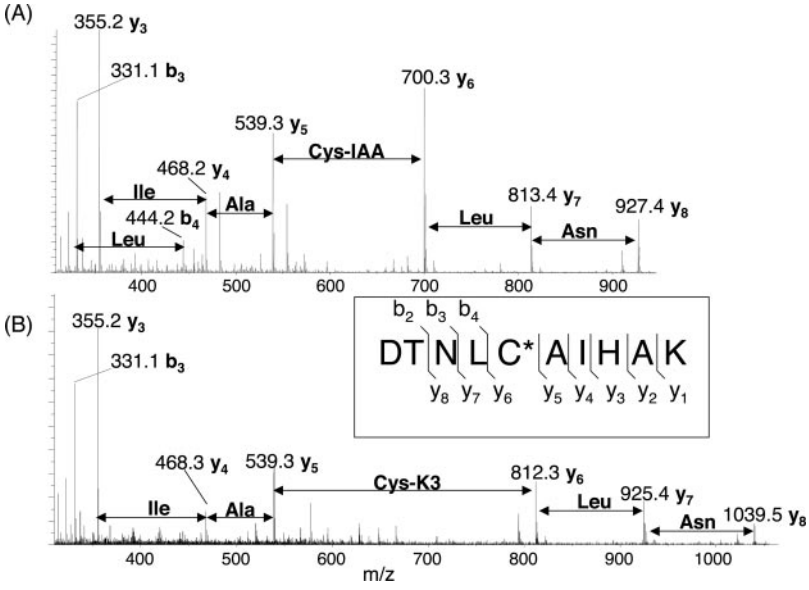

Fig. 8. Tandem MS identification of Cys110 modifications in treated histone H3.3/H3. LC-ESI-MS/MS analysis of the carboxymethylated 381.85^{+3} *m/z* peak (A) and the K3 adducted 419.17^{+3} *m/z* peak (B) from double digests of the treated histone preparations described in Fig. 7. A, fragmentation of the 381.85^{+3} *m/z* peak showing the 161 Da difference between the y_6 (700.3 *m/z*) and y_5 (539.3 *m/z*) ions and confirming the presence of a single IAA moiety coupled to Cys110 (Cys-IAA). B, fragmentation of the 419.17^{+3} *m/z* peak showing the 273 Da difference between the y_6 (812.3 *m/z*) and y_5 (539.3 *m/z*) ions and confirming the presence of a single K3 moiety coupled to Cys110 (Cys-K3). For both A and B data, b and y ions confirm the amino acid sequence, and the mass differences between y_5 and y_6 identify Cys110 as the modification site.

sulting from its arylating capacity and in vitro evidence identified Cys110 of histone H3/H3.3 as a potential target of K3 thiol arylation.

Site-specific phosphorylation is known to influence both k-8 organization and dynamics as well as to modulate k-8 interacting proteins (Liao et al., 1997; He et al., 2002; Ku et al., 2002; Schutte et al., 2004). Moreover, k-8 pSer73 formation in response to Fas receptor stimulation has been attributed to JNK activation (He et al., 2002). As shown here (Figs. 1–3), culture treatment of human breast cancer cells by K3 produced a rapid and sustained increase in k-8 pSer73 that was not mediated by JNK, p38, or P13K/Akt pathways because it was unaffected by their specific inhibitors, SP600125, SB203580, and LY294002, respectively. In contrast, K3-induced k-8 pSer73 was completely prevented by U0126, a specific inhibitor of MEK1/2, indicating that in MCF7, T47D, and SKBr3 cells, the MEK/Erk pathway mediates Ser73 phosphorylation of k-8 by the redox active and arylating quinone K3. It is noteworthy that culture treatment with the redox active but nonarylating quinone DMNQ produced only a marginal increase in intracellular k-8 pSer73, indicating that the arylating capability of K3 is largely responsible for its MEK/Erk-dependent phosphorylating effects on k-8. Furthermore, cotreatment of cultures with excess NAC completely prevented K3-induced phosphorylation of Erk1/2 and k-8. These observations are most consistent with the presence, within the enzymatic pocket of most signal-inhibiting phosphatases, of a conserved redox-sensitive cysteine residue that is also very sensitive to quinone-induced arylation (Klotz et al., 2002; Abdelmohsen et al., 2003).

Although activation of the Erk1/2 pathway by growth factors and other mitogens is often associated with cellular growth and survival, its aberrant or sustained activation has also been linked with cell death (Osada et al., 2001; Tikoo et al., 2001; Romashko et al., 2003; Choi et al., 2004; de Bernardo et al., 2004; Dong et al., 2004). Indeed, complete inhibition of Erk1/2 and k-8 phosphorylation by U0126 delayed the onset but did not ultimately prevent the resultant cytotoxicity produced by K3 (Fig. 3C). In contrast, cotreatment with excess NAC effectively prevented K3-induced cytoxicity, suggesting that arylation of intracellular targets apart from those involved in MAPK signaling predominantly determines K3-induced cytotoxicity. Morphologic and molecular characterization of K3-treated breast cancer cells during the 7 h leading to their complete loss of viability was consistent with a form of cell death known as oncosis, typically seen in response to toxic injury and with hallmarks that include generalized organelle swelling and loss of plasma membrane integrity (Trump et al., 1997; Van Cruchte and Van Den Broeck, 2002). Structurally intact k-8 filaments, relatively little genomic degradation with no DNA laddering, and an undistorted chromatin pattern on DAPI staining (Figs. 2, 3D, and 4), even after 3 h of K3 treatment, all pointed to an oncotic rather than apoptotic cell death process.

A novel result presented here was the demonstration that some cellular targets of K3 arylation, perhaps those more closely associated with its cytotoxic consequences, were readily visualized by fluorescence microscopy. Although the fluorescent properties of quinones are widely appreciated, we have found no reports describing induction of fluorescence upon the reaction of biologically relevant quinones like K3 with intracellular substrates. As is the case for a number of other thiol-modifying reagents, K3 thioether formation was shown to be associated with acquisition of enhanced K3 fluorescence, where excitation at wavelengths between 340 and 360 nm resulted in emission optima at wavelengths between 390 and 480 nm, depending on the chemical nature of the K3-arylated substrates (cysteine, glutathione, nuclear extract; Fig. 5). The K3 fluorescence properties illustrated by the in vitro fluorimetry measurements shown here may not fully represent all K3 reactions occurring in vivo; however, the concordance of these in vitro measurements with nuclear fluorescence imaged with excitation at 360 nm after K3 treatment of cultured breast cancer cells suggests that this in vivo fluorescence induction was a result of K3 thiol arylation. Cell cultures cotreated with U0126 showed no reduction in K3-induced nuclear fluorescence, whereas those cotreated with excess NAC showed complete inhibition of K3-induced fluorescence, indicating that this in vivo fluorescence was dependent on K3 arylation but was independent of its arylating induction of MAPK signaling. It is curious that studies with another well studied arylating agent, *p*-benzoquinone (BQ), demonstrated similar in vitro fluorescence induction on reaction with cysteine or glutathione substrates but no in vivo cellular fluorescence after BQ treatment of cultured cells, suggesting different in vivo permeability and/or chemical reactivity properties between BQ and K3 (data not shown). These apparent differences between the in vivo arylating properties of BQ and K3 could be further investigated using scanning electrochemical microscopy, because a recent study employed this approach to detect and monitor intracellular formation and efflux of the arylation product (thiodione) between K3 and glutathione in cultured hepatocytes (Mauzeroll et al., 2004).

Post-translational modifications to histones are crucial to the regulation and organization of chromatin structure, as has been extensively documented, and more recent interest has been shown in the use of mass spectrometry to delineate the full spectrum of histone modifications (Jenuwein and Allis, 2001; Berger, 2002; Syka et al., 2004). Histone H3 was implicated as a major target of intracellular K3 arylation from three initial observations: 1) K3-induced cellular fluorescence was observed to be predominantly nuclear; 2) in vitro fluorimetry of nuclear extracts showed enhanced fluorescence after K3 treatment; and 3) gel-separated proteins from K3-treated fluorescent nuclei revealed an abundant, UV transilluminated 17-kDa band aligning precisely with a Coomassie band confirmed by antibody and MS to be histone H3. As the only cysteine containing histone species, H3 and its variants all possess a core Cys110 residue that is evolutionarily conserved among metazoans (Sullivan et al., 2002). Some H3 variants, including the human H3.3 variants, contain an additional nearby cysteine residue (Sullivan et al., 2002). Functional and structural studies have demonstrated that the H3 core is buried within the nucleosomes when chromatin is in a closed configuration, protecting Cys110 from chemical modification (Arents et al., 1991; Bazett-Jones et al., 1996; Sun et al., 2002). When chromatin is in an open configuration, which is characteristic of actively transcribing genes, Cys110 is readily accessible for thiol adduction (Bazett-Jones et al., 1996; Sun et al., 2002). Employing ESI-MS/MS, in vitro studies confirmed that K3 reacts readily and

specifically with H3.3/H3, resulting in thiol arylation of its core Cys110 residue.

Taken together, these findings suggest that K3-induced cytotoxicity reflects oncosis primarily caused by the arylating property of this bifunctional quinone. Although k-8 pSer73 formation marked an early response to K3 treatment, K3-induced nuclear fluorescence coincided with the development of oncosis and the arylation of a 17-kDa nuclear protein identified as H3.3/H3. From recognition of the unique structural susceptibility of H3.3/H3, with its core Cys110 residue vulnerable to thiol arylation during active gene transcription, it may be speculated that H3.3/H3 also functions as a nuclear sensor of chemical stress.

Acknowledgments

We thank Dr. David Nichols and Danielle Crippen from the Buck Institute's Morphology Core for helpful advice and assistance.

References

Abdelmohsen K, Gerber PA, von Montfort C, Sies H, and Klotz LO (2003) Epidermal growth factor receptor is a common mediator of quinone-inducted signaling leading to phosphorylation of connexin-43: role of glutathione and tyrosine phosphatases. *J Biol Chem* **278:**38360–38367.

Arents G, Burlingame RW, Wang BC, Love WE, and Moundrianakis EN (1991) The nucleasomal core histone octamer at 3.1 Å resolution: a tripartite protein assembly and a left-handed superhelix. *Proc Natl Acad Sci USA* **88:**10148–10152.

Bazett-Jones DP, Mendez E, Czarnota GJ, Ottensmeyer FP, and Allfrey VG (1996) Visualization and analysis of unfolded nucleosomes associated with transcribing chromatin. *Nucleic Acids Res* **24:**321–329.

Berger SL (2002) Histone modifications in transcriptional regulation. *Curr Opin Genet Dev* **12:**142–148.

Bolton JL, Trush MA, Penning TM, Dryhurst G, and Monks TJ (2000) Role of quinones in toxicology. *Chem Res Toxicol* **13:**135–160.

Choi BK, Choi CH, Oh HL, and Kim YK (2004) Role of ERK activation in cisplatin-induced apoptosis in A172 human glioma cells. *Neurotoxicol* **25:**915–924.

Chou CF, Riopel CL, Rott LS, and Omary MB (1993) A significant soluble keratin fraction in 'simple' epithelial cells. *J Cell Science* **105:**433–444.

de Bernardo S, Canals S, Casarejos MJ, Solano RM, Menendez J, and Mena MA (2004) Role of extracellular signal-regulated protein kinase in neuronal cell death induced by glutathione depletion in neuron/glia mesencephalic cultures. *J Neurochem* **91:**667–682.

Dong J, Everitt JI, Lau SS, and Monks TJ (2004) Induction of ERK1/2 and histone H3 phosphorylation within the outer stripe of the outer medulla of the Eker rat by 2,3,4-tris-(glutathione-S-yl)hydroquinone. *Toxicol Sci* **80:**350–357.

Feng W, Liu G, Xia R, Abramson JJ, and Pessah IN (1999) Site-selective modification of hyperreactive cysteines of ryanodine receptor complex by quinones. *Mol Pharmacol* **55:**821–831.

He T, Stepulak A, Holmstrom TH, Omary MB, and Eriksson JE (2002) The intermediate filament protein keratin 8 is a novel cytoplasmic substrate for c-jun N-terminal kinase. *J Biol Chem* **277:**10767–10774.

Jenuwein T and Allis CD (2001) Translating the histone code. *Science (Wash DC)* **293:**1074–1080.

Klotz LO, Patak P, Ale-Agha N, Buchczyk DP, Abdelmohsen K, Gerber PA, von Montfort C, and Sies H (2002) 2-Methyl-1,4-naphthoquinone, vitamin K3, decreases gap-junctional intercellular communication via activation of the epidermal growth factor receptor/extracellular signal-regulated kinase cascade. *Cancer Res* **62:**4922–4928.

Ku NO, Azhar S, and Omary MB (2002) Keratin 8 phosphorylation by p38 kinase regulates cellular keratin filament reoganization: modulation by a keratin 1-like disease causing mutation. *J Biol Chem* **277:**10775–10782.

Liao J, Ku NO, and Omary MB (1997) Stress, apoptosis and mitosis induce phosphorylation of human keratin 8 at Ser-73 in tissues and cultured cells. *J Biol Chem* **272:**17565–17573.

MacDonald MJ, Husain RD, and Hoffmann-Benning S (2004) Immunochemical identification of coenzyme Q_0: dihydrolipoamide adducts in the E2 components of the α-ketoglutarate and pyruvate dehydrogenase complexes partially explains the cellular toxicity of coenzyme Q_0. *J Biol Chem* **279:**27278–27285.

Mauzeroll J, Bard AJ, Owhadian O, and Monks TJ (2004) Menadione metabolism to thiodione in hepatoblastoma by scanning electrochemical microscopy. *Proc Natl Acad Sci USA* **101:**17582–17587.

McKittrick E, Gafken PR, Ahmad K, and Henikoff S (2004) Histone H3.3 is enriched in covalent modifications associated with active chromatin *Proc Natl Acad Sci USA* **101:**1525–1530.

Osada S, Saji S, and Osada K (2001) Critical role of extracellular signal-regulated kinase phosphorylation on menadione (vitamin K3) induced growth inhibition. *Cancer* **91:**1156–1165.

Romashko J, Horowitz S, Franek WR, Palaia T, Miller EJ, Lin A, Birrer MJ, Scott W, and Mantell LL (2003) MAPK pathways mediate hyperoxia-induced oncotic cell death in lung epithelial cells. *Free Radic Biol Med* **35:**978–993.

Schmeider PK, Tapper MA, Kolanczyk RC, Hammermeister DE, Sheed BR, and Denny JS (2003) Discriminating redox cycling and arylation pathways of reactive chemical toxicity in trout hepatocytes. *Toxicol Sci* **72:**66–76.

Schutte B, Henfling M, Kolgen W, Bouman M, Meex S, Leers MPG, Nap M, Bjorklund V, Bjorklund P, Bjorklund B, et al. (2004) Keratin 8/18 breakdown and reorganization during apoptosis. *Exp Cell Res* **297:**11–26.

Seanor KL, Cross JV, Nguyen SM, Yan M, and Templeton DJ (2003) Reactive quinones differentially regulate SAPK/JNK and p38/HOG stress kinases. *Antioxid Redox Signal* **5:**103–113.

Sullivan S, Sink DW, Trout KL, Makalowska I, Taylor PM, Baxevanis AD, and Landsman D (2002) The histone database. *Nucleic Acid Res* **30:**341–342.

Sun JM, Chen HY, and Davie JR (2002) Isolation of transcriptionally active chromatin from human breast cancer cells using Sulfolink coupling gel chromatography. *J Cell Biochem* **84:**439–446.

Syka JE, Marto JA, Bai DL, Horning S, Senko MW, Schwartz JC, Ueberheide B, Garcia B, Busby S, Muratore T, et al. (2004) Novel linear quadrupole ion trap/FT mass spectrometer: performance characterization and use in the comparative analysis of histone H3 post-translational modifications. *J Proteome Res* **3:**621–626.

Tikoo K, Lau SS, and Monks TJ (2001) Histone H3 phosphorylation is coupled to poly-(ADP-ribosylation) during reactive oxygen species-induced cell death in renal proximal tubular epithelial cells. *Mol Pharmacol* **60:**394–402.

Toxopeus C, Holsteijn I, Thuring JW, Blaauboer BJ, and Noordhoek J (1993) Cytotoxicty of menadione and related quinones in freshly isolated rat hepatocytes: effects on thiol homeostasis and energy charge. *Arch Toxicol* **67:**674–679.

Trump BE, Berezesky IK, Chang SH, and Phelps PC (1997) The pathway of cell death: oncosis, apoptosis and necrosis. *Toxicol Pathol* **25:**82–88.

Van Cruchte S and Van Den Broeck W (2002) Morphological and biochemical aspects of apoptosis, oncosis and necrosis. *Anat Histol Embryol* **31:**214–223.

Address correspondence to: Dr. Christopher C. Benz, Program of Cancer and Developmental Therapeutics, Buck Institute for Age Research, 8001 Redwood Blvd., Novato, CA 94945. E-mail: cbenz@buckinstitute.org